Contrib Mineral Petrol (1991) 107:293–309

Contributions to Mineralogy and Petrology

Petrogenesis of the Merensky Reef in the Rustenburg section of the Bushveld Complex

D.M. Nicholson [1] * **and E.A. Mathez** [2]

[1] Department of Geological Sciences, University of Washington, Seattle, WA 98195 USA
[2] Department of Mineral Sciences, American Museum of Natural History, New York, NY 10024 USA

Received March 20, 1990 / Accepted October 26, 1990

Abstract. A petrogenetic model for the Merensky Reef in the Rustenburg section of the Bushveld Complex has been developed based on detailed field and petrographic observations and electron microprobe data. The model maintains that the reef formed by reaction of hydrous melt and a partially molten cumulate assemblage. The model is devised to account for several key observations: (1) Although the dominant rock type in the Rusterburg section is pegmatoidal feldspathic pyroxenite, there is a continuous range of reef lithology from pyroxenite to pegmatoidal harzburgite and dunite, and small amounts of olivine are present in nearly all pegmatoids. (2) The pegmatoid is usually bounded above and below by chromitite seams and the basal chromitite separated from underlying norite by a centimeter-thick layer of anorthosite. The thicknesses of the two layers exhibit a well-defined, positive correlation. (3) Inclusions of pyroxenite identical to the hanging wall and of leuconorite identical to the footwall are present in the pegmatoid. The leuconorite inclusions are surrounded by thin anorthosite and chromitite layers in the same sequence as that at the base of the reef. (4) Chromite in seams adjacent to plagioclase-rich rocks is characterized by higher Mg/Mg+Fe and Al/R3 and lower Cr/R3 than that in seams adjacent to pyroxene-rich rocks. Similar variations in mineral compositions are observed across individual chromitite seams where the underlying and overlying rock types differ. The chromite compositional variations cannot be rationalized in terms of either fractional crystallization or reequilibration with surrounding silicates. It is proposed that the present reef was originally a melt-rich horizon in norite immediately overlain by relatively crystallized pyroxenite. Magmatic vapor generated by crystallization of intercumulus melt migrated upward through fractures in the cumulate pile below the protoreef. The melt-rich protoreef became hydrated because fractures were unable to propagate through it and because the melt itself was water-undersaturated. Hydration of the intercumulus melt was accompanied by melting, and the hydration/melting front migrated downward into the footwall and upward into the hanging wall. In the footwall melting resulted first in the dissolution of orthopyroxene and then of plagioclase. With continued hydration chromite was stabilized as melt alumina content increased. The regular variations in chromite compositions reflect the original gradients in melt compositions at the hydration front. The stratigraphic sequence downward through the base of the reef of pegmatoid (melt) – chromitite – anorthosite – norite represents the sequence of stable mineral assemblages across the hydration/melting front. The sequence is shown to be consistent with knowledge gained from experiments on melting of hydrous mafic systems at crustal pressures. With cooling the hydrated mixture from partial melting of norite footwall and more mafic hanging wall crystallized in the sequence chromite-olivine-pyroxene-plagioclase, with peritectic loss of some olivine. Calculations of mass balance indicate that a significant proportion of the melt was lost from the melt-rich horizon. Variations in the development of the pegmatoid and associated lithologies and amount of modal olivine in the pegmatoids along the strike of the Merensky Reef resulted because the processes of hydration, melting and melt loss operated to varying extents.

* *Present address:* 2756 NE 103rd St., Seattle, WA 98125, USA
Offprint requests to: E.A. Mathez

Introduction

The Merensky Reef of the Bushveld Complex is a stratiform horizon of dominantly pegmatoidal feldspathic pyroxenite several tens-of-centimeters thick. It occurs within a cyclic sequence of orthopyroxenite to norite cumulates and is placed by most workers near the top of the Critical Zone (cf., Kruger and Marsh 1985). The Merensky Reef is famous for its enrichment in the platinum group elements (PGEs), and its remarkable regularity along many kilometers of strike has led to the general belief that both its geochemical character and strati-

graphic position were controlled by primary cumulate processes. Also it is recognized generally that strictly cumulate processes cannot account for the presence of pegmatoids or the close association with them of PGE mineralization. As pointed out by Lauder (1970), were the Merensky Reef a feature that cross-cut the igneous stratigraphy it would probably be viewed as hydrothermal. Petrogenesis appears to have involved modification of an originally cumulate sequence by hydromagmatic or subsolidus high-temperature hydrothermal processes.

Two questions are raised by these relationships: The first is why is PGE mineralization associated with pegmatoidal rocks. One group of workers has argued that the PGEs were concentrated by accumulation of magmatic suflides (e.g., Campbell et al. 1983) and that the formation of pegmatoids occurred by volatile influx subsequent to PGE concentration (Naldrett et al. 1986; Barnes and Campbell 1988). The opposing view is that vapor itself was responsible for transporting and concentrating the PGEs (Kinloch 1982; Ballhaus and Stumpfl 1986; Boudreau 1988). The question extends to the PGE-rich Howland (or J-M) Reef of the Stillwater Complex, and its resolution awaits specific data on the solubility of PGEs in complex, high-temperature fluids.

A second question is how did the stratiform pegmatoid horizons themselves form. Several such horizons exist in the Bushveld and Stillwater Complexes. Entrapment of volatiles in intercumulus melt below impermeable layers has been invoked by Jackson (1969) to account for the common association of pegmatoid with chromitite and by McCallum et al. (1977) to explain pegmatoidal troctolites at the bases of some of the anorthosite adcumulates in the Stillwater Complex; Lauder (1970) proposed that the Merensky Reef formed because the pyroxenite hanging wall served a similar purpose; and Boudreau et al. (1986) and Naldrett et al. (1986) pointed out that volatiles may have collected in the Howland and Merensky Reefs by dissolution in intercumulus melt. As far as the pegmatoids are concerned, Boudreau (1988) developed a model for petrogenesis of the Howland Reef which involved reaction of vapor with a protolith of norite and intercumulus melt to form the observed lithologic variations.

The point of the present investigation is to understand the petrogenesis of the Merensky pegmatoid and associated rocks in the Rustenburg section of Rustenburg Platinum Mines in the southwest sector of the Bushveld Complex. Eight stratigraphic sections through the Merensky Reef and immediately adjacent rocks were documented and sampled in detail. The rocks were studied petrographically and by electron microprobe. At Rustenburg the reef ideally is constituted as a pegmatoidal feldspathic pyroxenite bounded above and below by centimeter-thick layers of chromitite, with the lower chromitite separated from the footwall norite by a thin anorthosite layer. The association of these lithologies is the central problem of petrogenesis, and its explanation is the focus of this work. No observations have been made that bear on the question of how the PGEs became concentrated in the Merensky Reef, so this issue is not examined here.

General features of the Merensky Reef

The term "Merensky Reef" has had conflicting usage in the literature. Following the definition of Cousins (1964), here the term refers specifically to the pegmatoid and associated chromitite seams, to which we add also the basal anorthosite. Although PGEs are usually hosted by pegmatoid and chromitite, mineralization may also be concentrated in the footwall or hanging wall. The conflict in terminology has arisen because in mining usage "reef" refers to that which is mineralized or mined.

The Rustenburg section refers to the stratigraphy of the upper Critical Zone as exposed in the mines in the immediate vicinity of Rustenburg. The upper Critical Zone in this area has been described by Kruger and Marsh (1985) and Viljoen and Hieber (1986), and the Merensky Reef itself by Cousins (1969), Vermaak (1976), and Viljoen and Hieber (1986). Therefore, this description is limited to features deemed relevant to petrogenesis.

An idealized section of the Merensky Reef in the Rustenburg section is shown in Fig. 1. The pegmatoid is typically 10–30 cm thick and consists of coarse-grained (1–2 cm) bronzite and interstitial plagioclase with disseminated chromite. Phlogopite and sulfides are the dominant accessory minerals, and amphibole, zircon, rutile, magnetite, apatite, graphite and low-temperature alteration minerals such as talc, chlorite and serpentine have been reported (e.g., Ballhaus and Stumpfl 1985; Viljoen and Hieber 1986; Boudreau et al. 1986). In places the reef is harzburgitic. The bottom chromitite layer is typically 1–2 cm thick and the top seam thinner.

There are important departures from this idealized section in the Rustenburg and other "type sections". At Rustenburg the top chromitite seam may be represented by a mere dissemination, be absent altogether or occur slightly below rather than at the pegmatoid-pyroxenite contact (Cousins 1969), the bottom chromitite also may be developed poorly and three seams rather than the usual two may be present. In parts of the Impala (Leeb-du Toit 1986) and Western Platinum Mines (Farquhar 1986), which are adjacent to but on opposite sides of Rustenburg Mines, a well-developed pegmatoid layer is absent. Here the "reef" has been described as a pyroxenite with associated chromitite layers. However, for lack of detailed description it is not clear whether or not pegmatoids are completely missing from these sections. For example, at Western Platinum Mines Farquhar (1986) noted that the pyroxenite "tends to become pegmatitic" near the chromitite layers. At Atok in the eastern Bushveld chromitite seams and PGE mineralization are hosted by mixed pyroxenite+pegmatoid, which directly overlies a well-defined pegmatoid layer. Both regionally and locally in the vicinity of potholes the Merensky pegmatoid is of variable thickness. In the Rustenburg section, for example, the Reef reaches a thickness of almost 2 m near the Paardekraal shaft (Viljoen and Hieber 1986), and in the Union section it is over 7 m thick (Viljoen et al. 1986a). It is unlikely that the specific model developed for Rustenburg will be applicable throughout the Bushveld Complex.

The contact between the Merensky Reef and the footwall norite represents a break in the Bushveld sequence. Usually the contact is observed as a disconformity, being "dimpled" with undulations of 2–20 cm in amplitude. On a regional scale, the reef lies unconformably on the footwall rocks (Cousins 1969; Vermaak 1976). The contact is marked also by discontinuities in mineral compositions (Kruger and Marsh 1985) and initial Sr isotopic ratios (Kruger and Marsh 1982; Sharp 1985), suggesting that the level of the Merensky Reef marks an injection of new magma.

The Merensky Reef is found also in circular to elliptical depressions in the footwall known as potholes (Schmidt 1952; Viljoen and Hieber 1986; Viljoen et al. 1986a; Ballhaus 1988). The potholes are typically 30–250 m wide and up to 70 m deep (R.T. Brown, personal communication). Their floors are usually conformable to layering and present at certain lithologic breaks in the stratigraphy. At the flanks of some of them pegmatoid is absent and a single chromitite seam separates pyroxenite hanging wall and norite footwall. This chromitite (without pegmatoid) is termed "contact reef". In the bottoms of potholes the pegmatoid may

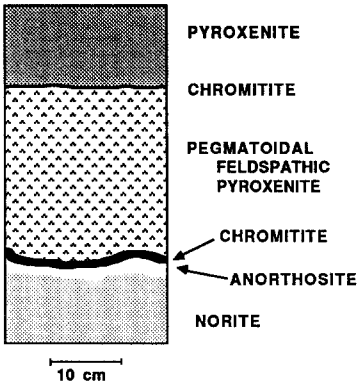

Fig. 1. Idealized section of the Merensky Reef in the Rustenburg section of the Bushveld complex. The reef consists of pegmatoidal feldspathic pyroxenite bound by chromitite seams, with the lower one separated from the footwall norite by a thin anorthosite layer. Sulfides (and their PGEs) typically are concentrated in the pegmatoid near the contacts with the chromitite seams

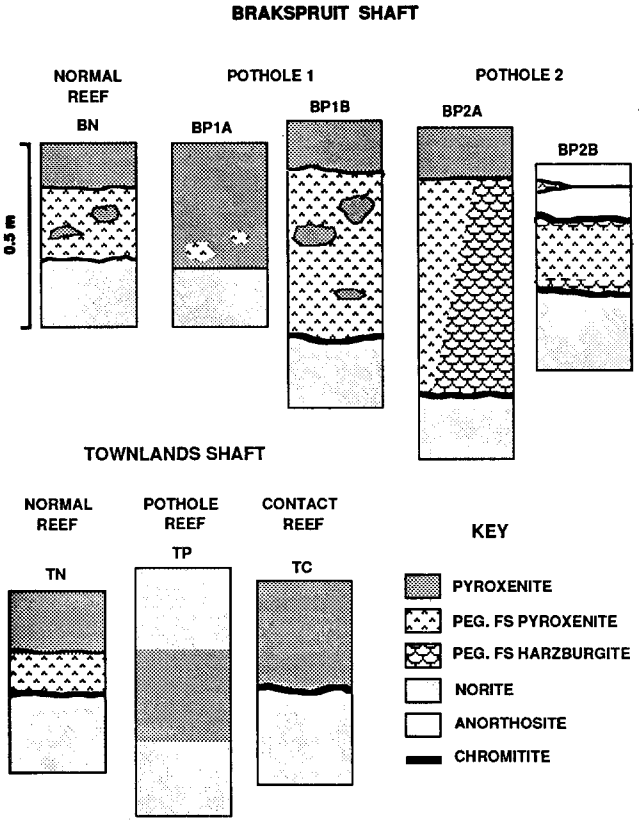

Fig. 2. Stratigraphic sections through the Merensky Reef in the Brakspruit and Townlands shafts, Rustenburg Platinum Mines

reappear bounded by the two chromitite seams, here termed "pothole reef". The latter is usually thicker and more olivine-rich than normal reef (Viljoen and Hieber 1986). There are systematic variations in PGE mineralization throughout the Merensky Reef, including the areas around potholes: In much of the normal reef PGEs are mostly in Pt-Pd sulfides, but in potholes Pt-Fe alloys dominate, in contact reef laurite is important and at pothole edges tellurides are relatively abundant (Kinloch 1982; Kinloch and Peyerl 1990).

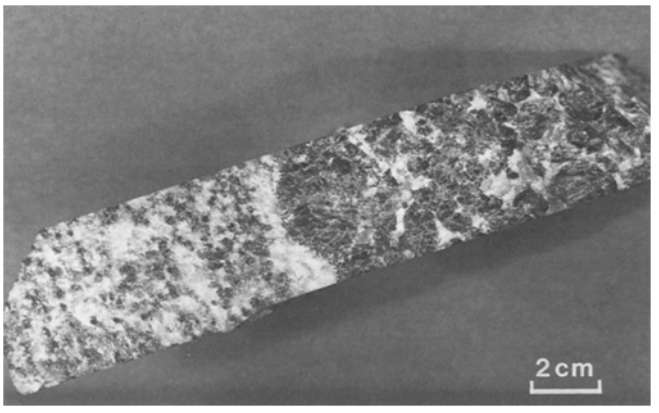

Fig. 3. Hand specimen of the Merensky pegmatoid (*right*), lower chromitite seam (at the pegmatoid – anorthosite contact), (*left*) anorthosite and underlying norite

The Merensky Reef of the Rustenburg section

Sampling and analytical procedures

Detailed stratigraphic sections were made of normal, pothole and contact reef at eight localities in the Brakspruit and Townlands shafts at Rustenburg Platinum Mines (Fig. 2). At each locality a vertical sequence of 8–10 samples was collected, spanning a range of 1–2 m below to about 1.5 m above the reef. The sampling was designed to recover as much of the stratigraphy and contact relationships as possible.

Approximately 120 polished sections were examined petrographically and used for electron probe study. The JEOL 733 probe at the University of Washington was used. Typical operating conditions were 15 keV acceleration potential and 30 nA sample current. Natural mineral standards of compositions similar to the unknowns and standard Bence-Albee correction procedures were used.

Rock types

Pegmatoidal feldspathic pyroxenite. The most common reef lithology in the Rustenburg section is pegmatoidal feldspathic pyroxenite (Fig. 3). A typical sample consists of 62% bronzite, 31% interstitial plagioclase, 3.6% chromite, and lesser amounts of clinopyroxene, phlogopite and hornblende. Plagioclase is interstitial to pyroxene, and the grain size is 0.5–1.5 cm. Traces of partially serpentinized olivine are present in nearly every thin section and usually occur as rounded cores in bronzite.

Chromite occurs as euhedral to subhedral grains in interstices and as inclusions in bronzite. As reported by Boudreau et al. (1986), phlogopite also occurs in two habits, namely as discrete grains with chromite in interstices between bronzite and plagioclase or replacing orthopyroxene, where it is associated with quartz. Sulfides occur as aggregates filling intersticies between pyroxene grains, as small blebs and inclusions in plagioclase and as <10-μm-diameter inclusions in planar arrays representing annealed fractures in plagioclase and orthopyroxene.

Pegmatoidal feldspathic harzburgite and dunite. Olivine-rich pegmatoid is common in potholes. One typical harzburgite is composed of 43% bronzite poikilitically enclosing 36% olivine, with 16% interstitial plagioclase. It also contains chromite (3%), sulfide (2%), phlogopite (1%) and hornblende (<1%). Rocks of up to 60% olivine are present, and in them modal bronzite correspondingly is low. The accessory mineral assemblage in the olivine-rich pegmatoids is similar to that in the olivine-poor ones.

Chromitite. The chromitites are typically composed of 40–50% euhedral to subhedral chromite and interstitial plagioclase or bronzite. Most individual grains are 50–250 μm across, but composite grains of up to 1500 μm in diameter also exist. Individual grains of the bottom chromitite seam tend to be slightly larger and more irregular in shape than those of the top seam. Orthopyroxene is the dominant interstitial mineral in the top chromitite seam and in the top third of the lower seam; plagioclase is interstitial in the lower two thirds of the lower seam. Additional description can be found in the works of Eales (1987) and Eales and Reynolds (1986).

Anorthosite. Underlying the basal chromitite seam is a relatively pure anorthosite (Fig. 3) composed of interlocking plagioclase grains 0.5–2 mm across. The rock contains several percent interstitial orthopyroxene and lesser amounts of clinopyroxene, but the interstitial minerals are restricted to localized patches. Small (0.2–0.5 mm) aggregate grains of interstitial sulfide are also present locally.

Footwall and hanging wall rocks. The footwall and hanging wall of the normal Merensky Reef are leuconorite (plagioclase-orthopyroxene cumulate; Fig. 3) and pyroxenite (orthopyroxene cumulate), respectively. The former is composed of 76% plagioclase and 19% orthopyroxene. Sparse olivine is present in the footwall within about 10 cm of the reef contact. Locally the footwall is weakly mineralized. The hanging wall pyroxenite is composed of 80% bronzite 2–3 mm across, 17% postcumulus plagioclase and scattered centimeter-size augite oikocrysts. Where oikocrysts are abundant locally the rock has a porphyritic appearance, and thus some literature descriptions refer to it as "porphyritic pyroxenite". Cumulus bronzite is corroded where it is in contact with the upper chromitite seam. Minor phases include sulfide (2.8%), hornblende (1%), phlogopite (<1%) and chromite (≪1%). The amount of interstitial plagioclase increases progressively upward until plagioclase becomes cumulus 1–1.5 m above the reef (Kruger and Marsh 1985).

Features of stratigraphy and lithology relevant to petrogenesis

Stratigraphic and lithologic variability. The sections of Fig. 2 illustrate the stratigraphic and lithologic diversity characteristic of the Merensky Reef. Thus, the BN section is in part composed of pegmatoidal feldspathic pyroxenite with inclusions of finer-grained pyroxenite (see below). The top chromitite seam in this section is discontinuous and in places represented only by slightly more disseminated chromite than in the pegmatoid. Here the top contact of the reef is sharp and defined by the contrast in grain size of the pegmatoid and pyroxenite. The TN section contains pegmatoidal feldspathic pyroxenite without pyroxenite inclusions, and both top and bottom chromitite seems and the anorthosite layers are well-developed. In one of the Townlands potholes, represented by section TP, the reef is absent altogether and fine-grained pyroxenite lies directly on leuconorite.

The reef lithologies are variable over distances of meters. This is observed, for example, in the BP2 pothole. On the one side of this pothole (section BP2A) pegmatoidal feldspathic pyroxenite grades into pegmatoidal harzburgite and dunite over a distance of two meters. Here the pegmatoid is sandwiched between well-developed top and bottom chromitite seems and the hanging wall and footwall are composed of the normal pyroxenite and norite, respectively. On the other side (section BP2B) the hanging wall is anorthosite rather than pyroxenite, and three chromitite seams are present. Two are located at their normal positions immediately above and below the pegmatoid; the third seam is located 10 cm above the pegmatoid in the overlying anorthosite. The reef pegmatoid here is feldspathic pyroxenite with relatively abundant phlogopite, but olivine is abundant only in the three chromitite seams and in the rocks immediately adjacent to them. For example, in the upper seam olivine forms the matrix in the middle of the seam and is replaced outward first by orthopyroxene and then plagioclase at the seam margins. The seam is locally bifurcated, with olivine occurring between its two branches.

In a second pothole, the section BP1B is similar to the nearby BN section. However, section BP1A is composed of fine-grained feldspathic pyroxenite similar to hanging wall pyroxenite except that it contains rare pegmatoidal orthopyroxene and is mineralized. A thin chromitite seam separates the pyroxenite from underlying leuconorite, but an intervening anorthosite is absent. A top chromitite seam is also absent. The stratigraphic and lithologic variability exhibited by the Merensky Reef is interpreted to reflect a progressive development of pegmatoid and associated lithologies, as discussed further below.

Association of anorthosite and chromitite. An anorthosite ("bleached zone") immediately underlying the basal Merensky chromitite (Fig. 3) is mentioned in descriptions of the Union (Viljoen et al. 1986a), Impala (Leeb-du Toit 1986), Rustenburg (Vermaak 1976; Viljoen and Hieber 1986; Ballhaus 1988), Western Platinum (Farquhar 1986) and Marikana sections (Brynard et al. 1976). The anorthosite generally is present beneath the chromitite of pothole, contact and normal reef. Where it has been observed by us it is concordant with chromitite and locally discordant to layering in the footwall, following the dips and swells of the dimpled contact. Elsewhere, however, the anorthosite is reported to be conformable to underlying norite and to pinch out around

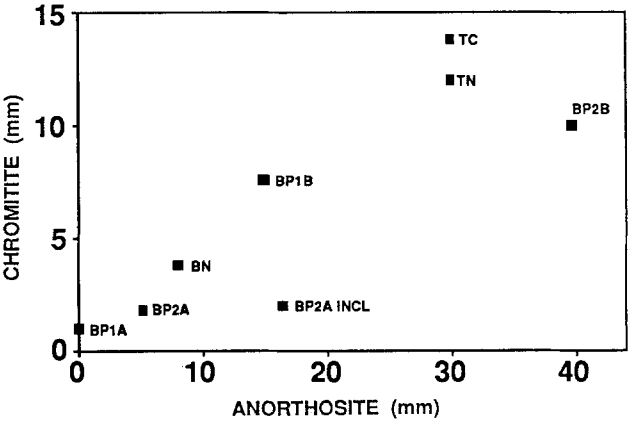

Fig. 4. The relationship between thickness of the basal chromitite seam and underlying anorthosite ("bleached zone") as measured in thin section

local dimples of the pegmatoid in the footwall (R.T. Brown, personal communication). The thickness of the two layers are clearly related (Fig. 4), and the association of the two rock types is regarded as a general feature of the Merensky Reef.

Norite and pyroxenite inclusions. Two types of inclusions have been found. Within pegmatoidal feldspathic pyroxenite are centimeter- to decimeter-size inclusions of pyroxenite identical in all respects, including texture, mode and mineral compositions, to hanging-wall pyroxenite. The contact between the two lithologies is sharp and sinuous. The inclusions are interpreted to be remnants of the hanging wall.

Two inclusions of norite identical to the footwall norite have also been found in the pothole represented by the BP2A section. The inclusions are 50 and 80 cm across and embedded in pegmatoidal feldspathic dunite. Variations in modal plagioclase and pyroxene define a layering in the inclusions which is slightly discordant to the regional layering of the footwall. The compositions of plagioclase and pyroxene in the norite inclusions are identical to those in the norite footwall and differ from those in the pegmatoid. Although they are rare, similar inclusions have been reported in other potholes (Viljoen and Hieber 1986), so the two described here are not an isolated occurrence. An important feature of the norite inclusions is that they are *completely* surrounded by an anorthosite layer 1–1.5 cm thick, which in turn is surrounded by 2–4 mm-thick chromitite layer. Thus, the sequence norite – anorthosite – chromitite – pegmatoid is the same as that of the basal contact of the Merensky Reef, suggesting that both formed by a similar process. The inclusions are interpreted to represent the protolith of the Merensky pegmatoid and the anorthosite and chromitite layers to have formed at a hydration/reaction front in the intercumulus melt (see below).

Occurrence of olivine. As noted above, olivine is present in at least trace quantities in nearly every pegmatoid and is usually more abundant in potholes than normal reef (Viljoen and Hieber 1986; Ballhaus 1988), some of the rocks in the former being essentially dunites. In the Amandelbult and Union sections olivine is more abundant than in the Rustenburg section, and the pegmatoids there are best termed feldspathic olivine pyroxenite to harzburgite (Viljoen et al. 1986a; Viljoen et al. 1986b). The ubiquity of olivine, the variability of its modal concentration, the gradation of olivine-free and olivine-rich rocks into each other and the expectation that olivine should have reacted out partially with cooling imply that it was initially much more abundant.

Table 1a. Representative analyses of minerals from the TN and BP2A sections of the Merensky Reef, Rustenburg section

Orthopyroxene

	T20 (+26.0)[a]	T18 (+9.0)	T18 (+6.8)	T18 (+6.7)	T18 (+4.5)	T18 (+0.8)	T18 (+0.5)	T18 (−3.1)	T-19 (−12.4)	B-15[d]	B-15[e]
SiO_2	54.76	54.59	53.38	54.98	54.53	55.01	55.69	54.99	54.38	54.4	55.3
TiO_2	0.18	0.20	0.15	0.23	0.15	0.11	0.09	0.31	0.29	0.14	0.01
Al_2O_3	1.28	1.38	1.73	1.33	1.70	1.49	1.03	1.10	1.18	1.44	0.18
Cr_2O_3	0.56	0.45	0.48	0.45	0.50	0.48	0.32	0.31	0.24	0.50	0
NiO	0.13	0.18	0.15	0.14	0.12	0.13	0.10	0.14	0.12	0.13	0.09
FeO[b]	11.94	13.15	12.23	12.13	11.14	10.18	8.81	14.21	14.32	12.76	13.06
MnO	0.26	0.30	0.29	0.25	0.23	0.25	0.20	0.30	0.33	0.30	0.32
MgO	28.52	29.14	28.94	29.66	30.39	31.01	32.31	28.63	27.69	30.22	31.04
CaO	2.68	0.77	1.03	0.90	0.92	0.80	0.39	0.88	1.06	0.93	0.63
Total	100.31	100.16	98.38	100.07	99.68	99.46	98.94	100.87	99.61	100.82	100.67
Si	1.951	1.948	1.936	1.954	1.938	1.950	1.966	1.957	1.962	1.929	1.962
Ti	0.005	0.005	0.004	0.006	0.004	0.003	0.002	0.008	0.008	0.004	0
Al	0.054	0.058	0.074	0.056	0.071	0.062	0.043	0.046	0.050	0.060	0.008
Cr	0.016	0.013	0.014	0.013	0.014	0.015	0.009	0.009	0.007	0.014	0
Fe^{2+}	0.356	0.392	0.371	0.360	0.331	0.302	0.260	0.423	0.432	0.378	0.387
Ni	0.004	0.005	0.004	0.004	0.003	0.004	0.003	0.004	0.003	0.004	0.003
Mn	0.008	0.009	0.009	0.008	0.007	0.008	0.006	0.009	0.010	0.009	0.010
Mg	1.515	1.550	1.565	1.571	1.611	1.638	1.701	1.519	1.489	1.597	1.641
Ca	0.102	0.029	0.040	0.034	0.035	0.030	0.015	0.034	0.041	0.035	0.024
Mg/Mg+Fe	0.810	0.798	0.808	0.813	0.829	0.845	0.867	0.782	0.775	0.809	0.809
Rock type[c]	Pyx	Pyx	Chr	Peg pyx	Peg pyx	Peg pyx	Chr	An	Nor	Peg pyx	Peg pyx

[a] T20(+26.0) = sample T20, 26 cm above base of lower chromitite in TN section
[b] All Fe as FeO
[c] Rock type: *Pyx* = pyroxenite; *Chr* = chromitite; *Peg* = pegmatoid; *An* = anorthosite; *Nor* = norite
[d] Crystal not included in olivine and
[e] inclusion in olivine in same thinsection, BP2A section
Additional data for the TN and other sections are presented in Nicholson (1989) and available from the authors

Mineral inclusions. Composite inclusions of phlogopite, amphibole and orthopyroxene are common in chromite in the chromitites but generally absent in chromite in the pegmatoids. Similar inclusions have been observed by Boudreau (1986) in the Stillwater Howland Reef. In addition, in several harzburgites orthopyroxene inclusions exist in olivine which itself is rimmed by orthopyroxene, giving the inclusion sequence pyroxene – olivine – pyroxene. The pyroxene-bearing inclusions also may contain phlogopite, muscovite and albite. The pyroxene rims and inclusions are not in optical continuity and, although they possess similar major element and Ni contents, the inclusions contain little Al, Ti and Cr (Table 1 a).

Table 1 a. (continued)

Plagioclase

	T20 (+30)	T18 (+1.8)	T18 (+0.3)	T18 (−0.5)	T19 (−12.0)
SiO_2	49.92	48.16	49.82	49.07	48.33
Al_2O_3	31.36	32.57	31.79	32.3	32.6
FeO	0.27	0.21	0.18	0.33	0.34
CaO	14.87	16.24	15.02	15.77	16.02
Na_2O	3.34	2.55	3.30	2.81	2.52
K_2O	0.25	0.13	0.17	0.17	0.15
Total	100.01	99.86	100.28	100.45	99.96
Si	2.284	2.214	2.272	2.240	2.219
Al	1.691	1.765	1.709	1.738	1.764
Ca	0.729	0.800	0.734	0.771	0.788
Na	0.296	0.227	0.292	0.249	0.224
K	0.015	0.008	0.010	0.010	0.009
Fe	0.010	0.008	0.007	0.013	0.013
An	0.701	0.773	0.709	0.749	0.772
Rock type	Pyx	Peg	Chr	An	Nor

Mineral chemistry

Plagioclase and orthopyroxene. As originally documented by Kruger and Marsh (1985), the base of the Merensky Reef marks discontinuities in plagioclase and orthopyroxene compositions. The relations are typified by the TN section (Fig. 5, Table 1 a). It can be seen that plagioclase in the pegmatoid is more sodic and exhibits greater compositional variability than that in the footwall norite. Plagioclase in the anorthosite falls within the compositional range of that in the underlying norite.

Orthopyroxene in the reef is chracterized by higher Mg/Mg+Fe and Al and Cr contents and lower Ti and Ni contents than that in the footwall. It becomes more magnesian in the top 10 cm of the footwall approaching the contact, but the trend is reversed upward through the pegmatoid. An exception to this general trend is exhibited in the TP section, where orthopyroxene compositions change from En_{81-83} in basal norite to En_{80-82} in pyroxenite to En_{77-78} in overlying norite. As noted above, the reef as defined here is missing (Fig. 2).

Table 1 a. (continued)

Chromite

	T18 (+6.6)	T18 (+5.1)	T18 (+4.1)	T18 (+2.2)	T18 (+1.8)	T18 (+0.7)	T18 (0)
SiO_2	0.06	0.06	0.07	0.06	0.06	0.02	0.04
TiO_2	2.58	1.06	1.19	1.64	1.13	0.78	1.58
Al_2O_3	11.63	14.86	15.17	13.00	15.10	17.20	16.21
Cr_2O_3	38.90	41.24	38.06	38.14	40.07	39.89	40.04
Fe_2O_3	15.39	11.97	14.74	14.82	12.01	11.12	11.99
NiO	0.42	0.22	0.20	0.23	0.19	0.15	0.28
FeO	25.97	23.60	23.97	25.58	22.87	21.49	22.60
MnO	0.37	0.35	0.34	0.39	0.36	0.30	0.37
MgO	6.66	7.57	7.53	6.21	7.85	8.82	8.80
Total	101.97	100.93	101.28	100.07	99.64	99.77	101.91
Si	0.002	0.002	0.002	0.002	0.002	0.001	0.001
Ti	0.064	0.026	0.029	0.042	0.028	0.019	0.038
Al	0.456	0.575	0.585	0.516	0.589	0.659	0.613
Cr	1.022	1.070	0.985	1.016	1.048	1.026	1.016
Fe^{3+}	0.385	0.296	0.363	0.376	0.299	0.272	0.289
Ni	0.011	0.006	0.005	0.006	0.005	0.004	0.007
Fe^{2+}	0.722	0.648	0.656	0.721	0.633	0.585	0.606
Mn	0.010	0.010	0.009	0.011	0.010	0.008	0.010
Mg	0.330	0.370	0.367	0.312	0.387	0.428	0.421
Al/R3	0.245	0.296	0.303	0.271	0.304	0.337	0.320
Cr/R3	0.549	0.551	0.509	0.532	0.541	0.524	0.530
Fe^{3+}/R3	0.207	0.152	0.188	0.197	0.154	0.139	0.151
Rock type	Chr	Peg pyx	Peg pyx	Peg pyx	Chr	Chr	Chr

The shift to more magnesian pyroxene from the norite to overlying rocks has been attributed by Barnes (1986) to the "trapped liquid shift." It is anticipated that cumulus orthopyroxene becomes progressively enriched in iron and depleted in compatible trace elements (e.g., Cr) as the amount of intercumulus melt with which it reacts increases. Thus, Barnes interpreted the compositional difference between norite pyroxene and pyroxenite pyroxene to reflect an initially higher proportion of intercumulus melt in the former. Although the petrogenetic model proposed below calls on just such a difference in proportions of intercumulus melt between the pyroxenite and norite protoliths of the Merensky Reef, other factors also influence pyroxene composition. In particular, orthopyroxene in massive chromitite is usually more magnesian than orthopyroxene in other rock types (e.g., Irvine 1967; Hatton and von Gruenewaldt 1985). This is evident as well in the Merensky rocks. In the TN section, for example, the average orthopyroxene composition in chromitite is $En_{85.7}$, but in the adjacent pegmatoid it is $En_{83.2}$. The compositional variations with mode are interpreted to be due in part to continued reequilibration of orthopyroxene and chromite with cooling (see below).

Table 1a. (continued)

Phlogopite

	T20 (+30.0)	T18 (+0.3)	T18 (−2.8)	T22 (−55.0)
SiO_2	39.75	38.75	37.30	37.77
TiO_2	3.19	4.32	3.84	3.11
Al_2O_3	13.42	13.35	12.90	12.84
Cr_2O_3	0.84	1.01	0.96	0.71
FeO	7.93	2.94	11.39	12.85
MnO	0.05	0.02	0.11	0.09
MgO	20.43	22.41	17.18	16.28
Na_2O	0.05	0.39	0.03	0.03
K_2O	10.07	9.55	9.88	9.61
Cl	0.32	0.15	0.46	0.65
F	0.30	0.58	0.13	0
BaO	0.23	0.25	0.32	0.38
Subtotal	97.08	93.72	94.49	94.32
H_2O	3.91	3.91	3.87	3.86
O=Cl,F	0.20	0.28	0.16	0.15
Total	100.79	97.35	98.2	98.04
Si	5.714	5.636	5.621	5.724
Ti	0.345	0.472	0.435	0.355
Al	2.274	2.289	2.292	2.293
Cr	0.096	0.116	0.114	0.085
Fe	0.953	0.358	1.435	1.628
Mn	0.006	0.002	0.014	0.012
Mg	4.379	4.860	3.859	3.679
Na	0.014	0.110	0.008	0.100
K	1.938	1.773	1.899	1.858
Cl	0.077	0.036	0.116	0.167
F	0.137	0.268	0.063	0
Ba	0.013	0.014	0.019	0.023
H_2O	3.786	3.696	3.821	3.833
Rock type	Pyx	Chr	An	Nor

Olivine. The composition of olivine in harzburgite and dunite is Fo_{78-80} and in pegmatoidal feldspathic pyroxenite is Fo_{80-82} (Table 1b). No systematic variations with stratigraphic position were found. Olivine typically contains 0.40–0.55 wt% NiO but exhibits depletions in Ni at grain boundaries, particularly where it is in contact with sulfide (NiO ≈ 0.23%). The distribution of Ni between olivine (ol) and sulfide (s) is described by the exchange reaction (e.g., Fleet and MacRae 1988)

$$FeS_{(s)} + NiSi_{0.5}O_{2(ol)} = NiS_{(s)} + FeSi_{0.5}O_{2(ol)}, \quad (1)$$

for which the equilibrium constant (K), assuming ideal solutions, is

$$K = (X^{s}_{Nis})\,(X^{ol}_{FeSi_{0.5}O_2})/(X^{S}_{FeS})\,(X^{ol}_{NiSi_{0.5}O_2}).$$

Data are lacking on the composition of the bulk sulfide at Rustenburg. In the neighboring Impala Mine the molecular Ni/Fe of sulfide is 0.282 (Mostert et al. 1982), which when combined with the Rustenburg olivine data

Table 1b. Representative analyses of olivine from various sections through the Merensky Reef of the Rustenburg section

	BP2A (+28.6)	BP2A (+15)	BP2A (+8)	BP2A (+1.2)	TC (−15)	BP2B (+22.2)	BP2B (+20)	BP2B (−3.4)
SiO_2	38.84	38.61	38.82	38.7	38.29	38.91	39.35	38.27
NiO	0.55	0.47	0.51	0.42	0.45	0.42	0.45	0.36
FeO	19.79	19.64	19.88	17.93	20.85	21.65	17.41	22.08
MnO	0.29	0.25	0.25	0.25	0.32	0.26	0.17	0.25
MgO	40.29	40.63	40.91	41.89	39.15	39.64	42.52	39.01
Total	99.76	99.60	100.37	99.19	99.06	100.95	99.95	100.07
Si	1.002	0.998	0.996	0.996	1.001	1.000	1.001	0.996
Fe	0.427	0.424	0.427	0.386	0.456	0.465	0.370	0.480
Ni	0.011	0.010	0.011	0.009	0.009	0.009	0.009	0.008
Mn	0.006	0.005	0.005	0.005	0.007	0.006	0.004	0.006
Mg	1.550	1.565	1.565	1.608	1.526	1.519	1.613	1.513
Fo	0.784	0.787	0.786	0.806	0.770	0.765	0.813	0.759
Rock type	Peg	Peg	Peg	Peg	Nor	Peg	Peg	Nor

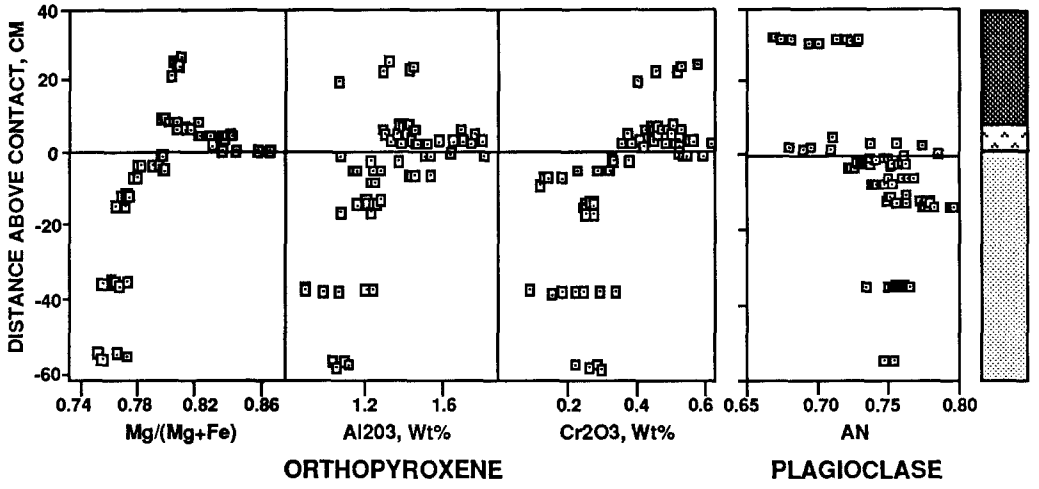

Fig. 5. Orthopyroxene and plagioclase compositional variations through the Merensky Reef in the TN section. The key to rock types is given in Fig. 2

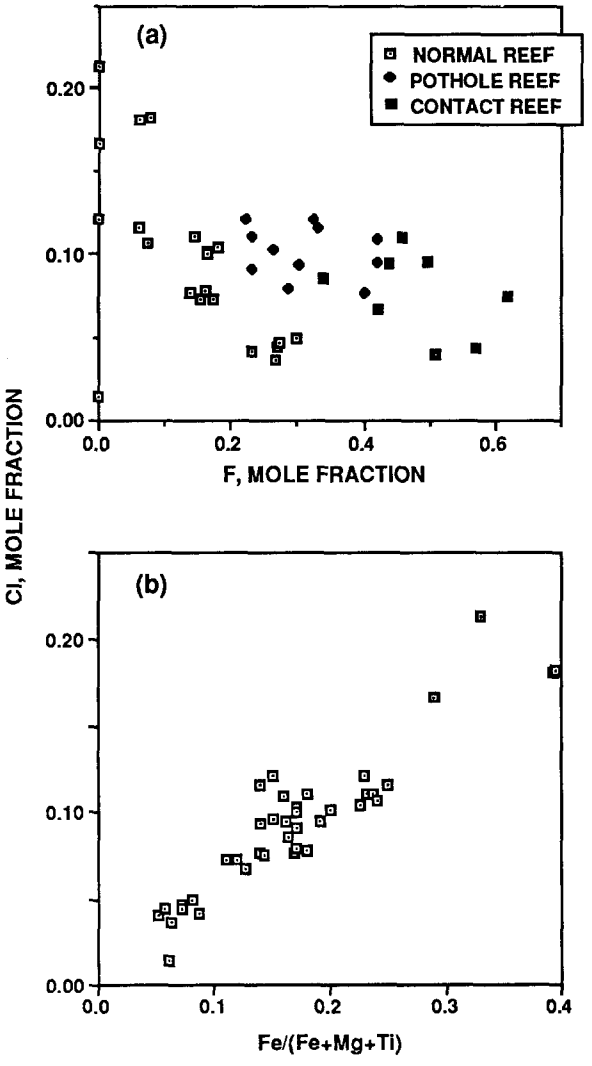

Fig. 6. **a** Halogen contents of phlogopite in normal and pothole reef in the Townlands shaft. Note that phlogopite in pothole reef is enriched in F compared to that in normal reef. **b** The variation of Cl contents of phlogopite as a function of Fe/(Fe+Mg+Ti). Phlogopite F contents exhibit no correlation with either Fe/(Fe+Mg+Ti) or Si/(Si+Al)

yields values of K of 11.1 and 20.3 for corresponding olivine core and rim compositions of 0.55 and 0.23 wt% NiO, respectively. The former is similar to the K of 9.7 ± 1.4 determined by Barnes and Naldrett (1985) for sulfide/olivine pairs in the Stillwater Howland Reef but differs from Ks of ≈30 obtained in the experiments of Fleet and MacRae (1988).

Phlogopite. Phlogopite in potholes is relatively enriched in F compared to that in normal reef, but there is no accompanying difference in Cl contents (Fig. 6a). The amounts of F and Cl that can be incorporated into phlogopite are strongly influenced by its Fe/(Fe+Mg+Ti) and Si/(Si+Al) ratios (e.g., Volfinger et al. 1985). However, while the Cl contents and Fe/(Fe+Mg+Ti) of Merensky phlogopite are clearly correlated (Fig. 6b), F contents are independent of that or any other compositional parameter (cf. Boudreau et al. 1986). The variable F contents of phlogopite are interpreted to be due to compositional variability of isolated pockets of intercumulus melt. This implies that the intercumulus melt in potholes was of generally different composition from that in normal reef (Fig. 6a). The amount of Cl in the phlogopite is interpreted to have been controlled by continued reaction of phlogopite with vapor during cooling through a wide subsolidus temperature interval, with the reaction involving mainly exchange of Cl rather than F.

Although phlogopite is not common in the footwall, the few grains that have been located in it are essentially F-free. Thus, the reef marks a sharp discontinuity in phlogopite F contents. The higher F content of the reef phlogopite is interpreted to indicate that it grew in the presence of a higher proportion of intercumulus melt. Representative analyses of phlogopite from the TN section are included in Table 1a.

Chromite. Compositional variations of chromite with stratigraphic position are illustrated for the TN section

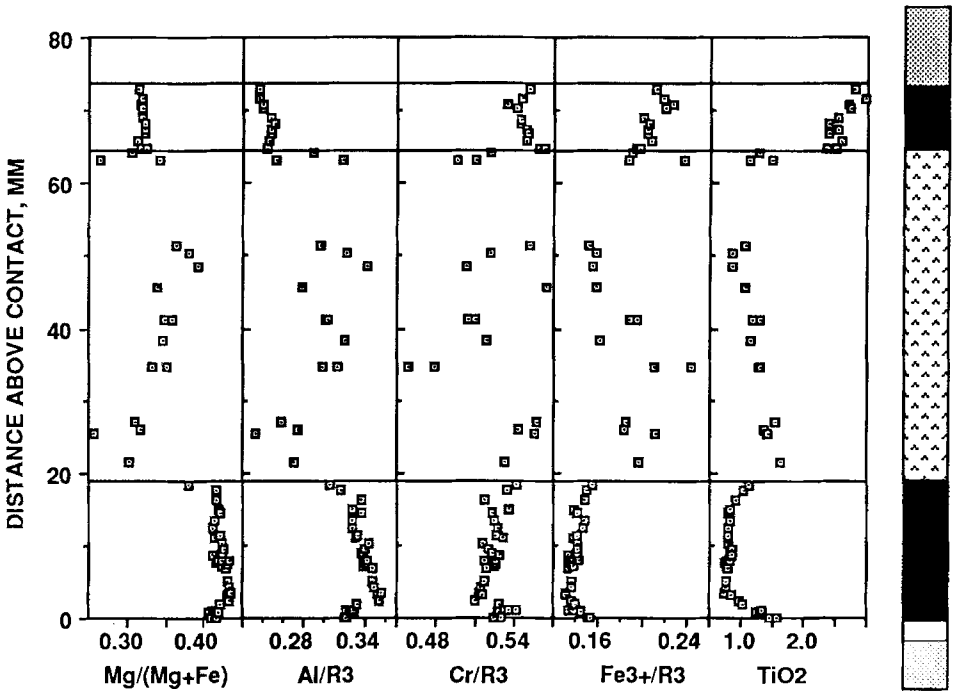

Fig. 7. Variation in chromite composition in the TN section. Similar variations have also been observed in other sections. See also Table 2. The key to rock types is given in Fig. 2

Table 2. Systematics of chromite compositions in various rock types

Section	Layer	Adjacent rock	Al/R3	Cr/R3	Mg/(Mg+Fe)
TN	Top chr[a]	Peg, pyx	0.254±0.004	0.559±0.008	0.310±0.003
	Peg		0.301±0.042	0.547±0.039	0.325±0.055
	Basal chr	Nor, peg	0.348±0.011	0.540±0.007	0.401±0.011
BN	Top chr	Peg, pyx	0.197±0.010	0.620±0.015	0.205±0.009
	Peg		0.220±0.053	0.610±0.032	0.198±0.097
	Basal chr	Nor, peg	0.281±0.013	0.564±0.016	0.317±0.013
BP1B	Top chr	Peg, pyx	0.317±0.010	0.590±0.016	0.329±0.014
	Peg		0.296±0.066	0.642±0.061	0.293±0.073
	Basal chr	Nor, peg	0.355±0.005	0.574±0.007	0.337±0.007
BP2B	Top chr	An	0.350±0.006	0.486±0.010	0.293±0.011
	Middle chr	Peg, an	0.346±0.009	0.507±0.011	0.307±0.015
	Peg		0.268±0.066	0.595±0.058	0.233±0.080
	Basal chr	Nor, peg	0.354±0.006	0.524±0.008	0.349±0.008

[a] Abbreviations as in Table 1

(Fig. 7), and representative analyses are presented in Table 1a. Similar relations are observed in other sections. Four features of the data are apparent:

1. Chromite in the pegmatoid exhibits a wide compositional range compared to chromite in individual chromitite seams. This has also been observed elsewhere in the Bushveld complex (Cameron and Desborough 1969; Hatton and von Gruenewaldt 1985).
2. There are distinct differences in average chromite compositions from one chromitite seam to another. These differences are systematically related to the nature of the adjacent rock type (Table 2). Chromite in seams adjacent to plagioclase-rich rocks possesses higher Mg/Mg+Fe and Al/R3 and lower Cr/R3 than chromite in seams adjacent to pyroxene-rich rocks.
3. Across individual seams there are systematic variations in chromite compositions. Again, this is related to the lithology of the adjacent rock type, with Mg/Mg+Fe and Al/R3 increasing and Cr/R3 decreasing progressively toward plagioclase-rich rocks (cf., Henderson and Suddaby 1971). For example, in the TN section (Fig. 7) the lower chromitite, which is bound by pegmatoidal pyroxenite above and anorthosite below, is characterized by a downward trend of increasing Mg/Mg+Fe and Al/R3 and decreasing Cr/R3. This compositional trend is not related to stratigraphic direction. Thus, the middle chromitite seam of the BP2P section, which is overlain by anorthosite (Fig. 2), exhibits a similar, upward trend.
4. The general compositional trend of chromite across chromitite seams is reversed within about 3 mm of the contact between the lower chromitite and underlying anorthosite (Fig. 7).

Controls on chromite composition. The interpretation of chromite compositional trends is complicated by crystal-chemical effects. The strong correlations of Al and Mg and of Cr and Fe^{2+} and antipathetic correlation of Al and Cr observed in chromite in this and other studies in part reflect the intracrystalline-exchange equilibrium (Sack 1982; Hill and Sack 1987),

$$FeAl_2O_4 + MgCr_2O_4 = MgAl_2O_4 + FeCr_2O_4, \quad (2)$$

for which the position of equilibrium lies far to the right. Therefore, reciprocal-exchange substitution occurs mainly between the components $FeCr_2O_4$ and $MgAl_2O_4$. This behavior is most clearly illustrated by submarine basalt glasses (Fisk and Bence 1980; Allan et al. 1988). In them Al, Mg and Fe contents of chromite and coexisting glass are strongly correlated, but no similar correlation exists for Cr. Thus, as plagioclase crystallizes melt Al content and chromite Al/R3 decrease, forcing chromite Cr/R3 to increase and countering the effect of chromite crystallization on Cr/R3. (That plagioclase appeared somewhat earlier in the Bushveld than in the Stillwater paragenetic sequence must be among the reasons that Bushveld Upper Critical Zone chromitites are more Cr-rich than Stillwater Ultramafic Zone chromitites.)

There are at least three processes that potentially could have affected chromite composition in the Merensky Reef. The first is fractional crystallization. Had this been important top-seam chromite would contain less Mg and Cr and more Al, Fe^{3+} and Ti than bottom-seam chromite due to crystallization of chromite and pyroxene (the "cumulate" minerals in the Merensky sequence), and within individual seams chromites would exhibit consistent upward increases in Al and Mg and decreases in Cr and Fe contents. Such relationships are not observed (Table 2; Fig. 7).

A second possibility is that chromite experienced extensive postcumulus or even subsolidus reequilibration. It has been observed repeatedly that Mg/Mg+Fe of chromite *and* mafic silicate minerals in chromitites are higher than these ratios of the corresponding minerals of adjacent silicate-rich rocks (e.g., Irvine 1967; McCallum 1968; Jackson 1969; Cameron and Desborough 1969; Henderson and Suddaby 1971; Hamlyn and Keays 1979; Eales and Reynolds 1986). There is ample evidence for Fe-Mg exchange between chromite and mafic silicate minerals. For chromite-orthopyroxene the exchange may be written (Irvine 1967),

$$MgY_2O_4 + FeSiO_3 = FeY_2O_4 + MgSiO_3 \quad (3)$$

(Y=Cr, Al or Fe^{3+}), the equilibrium constant of which increases with cooling. The systematic differences in mineral compositions with lithology, at least for Fe-Mg, result because in chromitites chromite dominates reaction (3) whereas in silicate-rich rocks pyroxene domiantes it.

If chromite compositions are controlled by subsolidus reactions, then there must be other minerals with which chromite exchanges Al and Cr. One possibility is orthopyroxene (Eales and Reynolds 1986):

$$MgAlO_4 + FeAlCrSiO_6 = FeCr_2O_4 + MgAl_2SiO_6. \quad (4)$$

However, there is no evidence that reaction (4) occurred in the Merensky rocks: (1) No systematic variation in orthopyroxene Al/Al+Cr corresponding to that in Mg/Mg+Fe exists. (2) The zoning in orthopyroxene in contact with chromite is such that Mg/Mg+Fe and Cr/R3 increase and Al/R3 decreases toward the contact (Fig. 8). This pattern is consistent with that predicted by reaction (3) but in the opposite sense of that predicted by (4). (3) There is no systematic relationship between chromite composition and the nature of the adjacent silicate phase.

Although the evidence does point to some Fe-Mg exchange between chromite and orthopyroxene, strictly subsolidus processes cannot account for the compositional variations of chromitite seams or the trends across them because there is no evidence for Al-Cr exchange. The problem has been recognized by other students of layered intrusions (Henderson 1975; Hamlyn and Keays 1979; Eales and Reynolds 1986), and thus it has been proposed that melt was also involved in reactions with chromite. For example, a general peritectic reaction has been invoked:

Mg-Fe-Al-Cr spinel + melt → Fe-Cr spinel + anorthite + forsterite (or enstatite).

Such a reaction could explain the trend to more evolved chromite compositions at the immediate contact of the lower chromitite seam with underlying anorthosite (Fig. 7). However, it offers no obvious explanation for the other compositional relations noted above.

This brings us to a third possibility, namely that the compositional variations in Merensky chromites reflect isothermal compositional gradients in intercumulus melt. This is developed in the following section.

Petrogenesis

Summary of relevant observations

The lithologic and mineralogic features of the Merensky Reef judged to be important for development of a petrogenetic model are summarized as follows:

1. The Merensky Reef is essentially a pegmatoid. Although detailed descriptions are lacking, it appears that even where the reef is dominantly fine-grained pyroxenite pegmatoids are present.
2. Chromitite seams occur at the contacts between the pegmatoid and the underlying and overlying finer-grained rocks. Chromitite and pegmatoid are associated, even where fine-grained pyroxenite is the dominant rock-type.
3. Over much of its strike length the reef rests on a disconformity with underlying rocks.
4. A layer of pure anorthosite is usually present beneath the lower chromitite (Fig. 3), and the thicknesses of the two layers are related (Fig. 4).
5. There is a continuous range in reef lithology from pegmatoidal feldspathic pyroxenite to harzburgite and dunite. Most rocks contain at least small amounts of olivine, suggesting that olivine was more abundant initially.

6. Inclusions of fine-grained pyroxenite identical to the hanging wall pyroxenite are present in the pegmatoid.
7. The pegmatoid also contains inclusions of leuconorite identical to the footwall norite. The inclusions are rimmed by thin anorthosite and chromitite layers in a sequence identical to that at the contact of the pegmatoid and footwall norite.
8. Plagioclase is more sodic and orthopyroxene more magnesian in the pegmatoid than in underlying rocks. A similar discontinuity in mineral composition does not exist between the pegmatoid and overlying pyroxenite (Fig. 5).
9. Chromite in chromitite seams adjacent to plagioclase-rich rocks possesses higher Mg/Mg+Fe and Al/R3 and lower Cr/R3 than chromite in seams adjacent to pyroxene-rich rocks. A similar relationship is observed in chromite compositional trends across individual seams where overlying and underlying rock types differ (Fig. 7; Table 2). The chromite compositional variations cannot be rationalized in terms of either fractional crystallization or postcumulus reequilibration.

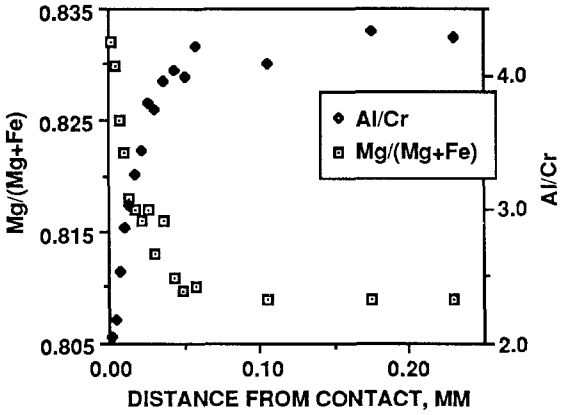

Fig. 8. Zoning in orthopyroxene adjacent to an inclusion of chromite. The pattern is opposite to that suggested by reaction (4), and the amount of exchange required to produce the observed zoning has an insignificant effect on chromite composition. Sample B15, section BP2A

Petrogenetic model

These observations are used to develop a model for the formation of the Merensky pegmatoid and associated lithologies by a secondary, hydromagmatic process analogous to that proposed by Boudreau (1988) for the Howland Reef of the Stillwater Complex. The hypothesis maintains that the reef formed by the melting of a partially molten protolith due to hydration. Its details are as follows:

The Merensky protoreef and introduction and evolution of vapor. The protoreef is taken to be partially molten norite overlain by pyroxenite containing a much smaller proportion of partial melt, as illustrated on the left-hand side of Fig. 9. How such a horizon originated is unclear. However, the existence of variations in proportions of intercumulus melt in cumulate sequences is suggested by the stratigraphic variations in mode, grain size and mineral compositions in the Bushveld and other intrusions (e.g., Barnes 1986).

Volatiles were introduced to the melt-rich horizon as vapor via a series of high-angle fractures in underlying rocks. Compaction may produce cumulates having only small quantities of intercumulus melt (Walker et al. 1988), so such rocks should support brittle deformation under a relatively wide range of stress conditions. Vapor was concentrated in the melt-rich zone because the zone could not sustain fractures, which therefore were unable to propagate further upward. It is tempting to suppose that the loci of fractures that supplied vapor are now marked by potholes. This possibility is consistent with this model and is discussed further below.

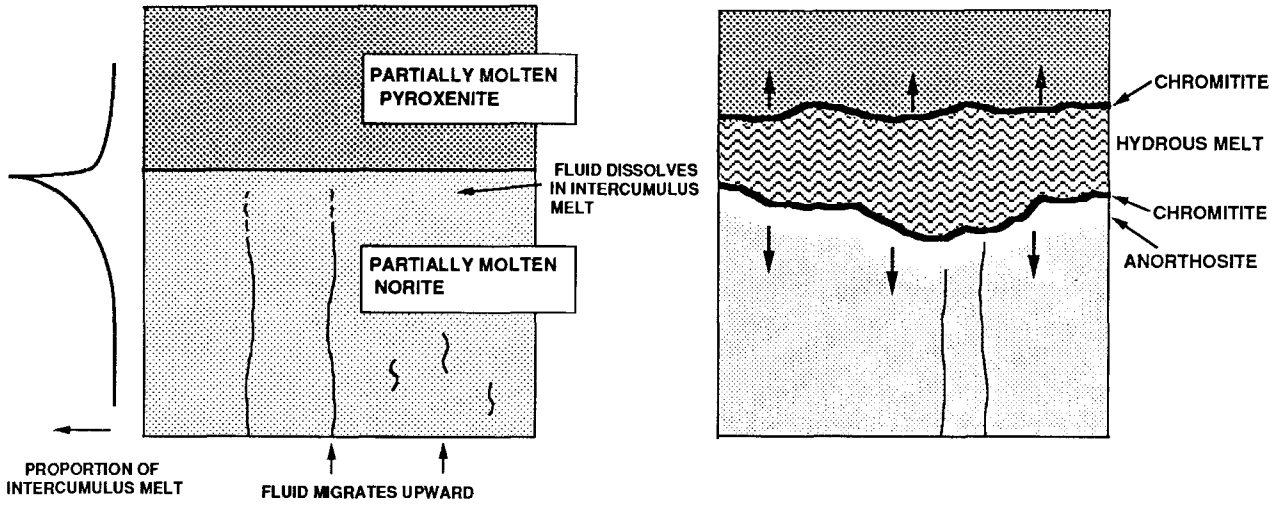

Fig. 9. Model for development of the Merensky Reef. The protoreef consisted of a melt-rich horizon of norite overlain by pyroxenite *Left*, the relative proportion of partial melt is indicated. Vapor migrated upward through Critical Zone rocks through fractures, which were unable to propagate through the melt-rich zone. The melting/hydration front moved downward into the footwall norite, where anorthosite and chromitite seams formed, and upward into the hanging wall pyroxenite, where a chromitite seam formed

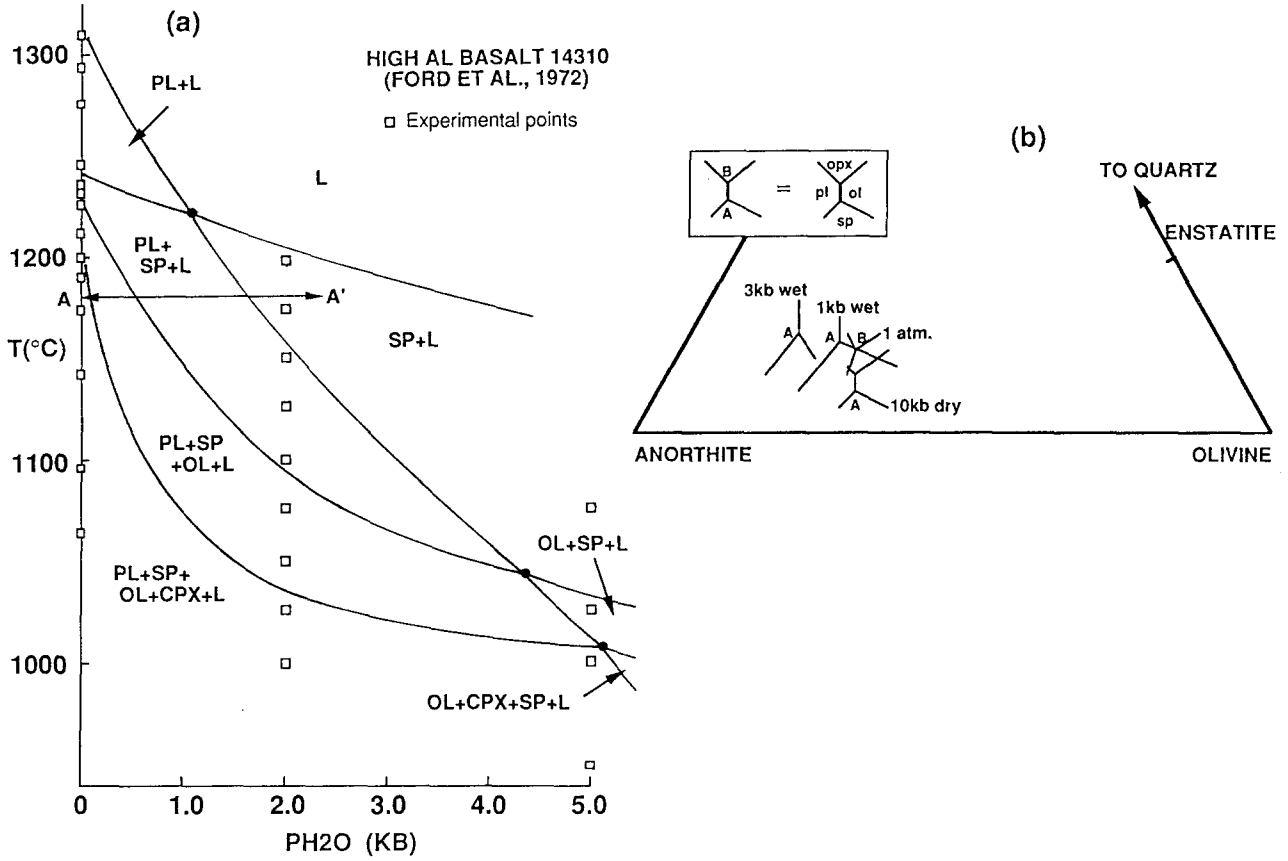

Fig. 10. a Near-liquidus phase relations of Apollo 14 high-alumina basalt 14310 redrawn from the data (*squares*) of Ford et al. (1972). Phase relations at near-solidus temperatures are omitted for simplicity. Note that spinel is stabilized relative to other minerals with increased P_{H_2O}. Note also that the effect of increasing P_{H_2O} from 1 atm to 2 kbar at a constant temperature of 1175° C (path *A–A'*) results in dissolution of the crystalline phases in the order pyroxene – olivine – plagioclase – spinel. **b** The effects of water and pressure on the liquidus relations of high-alumina basalt projected from "diopside" onto the olivine – plagioclase – silica plane of O'Hara (1968). After Ford et al. (1972; Fig. 8)

The melt-rich protoreef also acted as an impermeable barrier to the flow of water because it was initially anhydrous (Naldrett et al. 1986; Barnes and Campbell 1988). Hydration of the melt as it came in contact with vapor must have been accompanied by change in vapor composition. At pressure the solubility of water in silicate melt is much greater than that of the carbon species, so vapor in equilibrium with melt is constrained to be carbon-rich. For example, it has been estimated that in submarine basalts $(CO_2/H_2O)_{vapor}/(CO_2/H_2O)_{melt} \approx 450$ (Mathez 1989). In consequence, H_2O-rich vapor (i.e., >20% H_2O) could have evolved from the underlying cumulate sequence only if the vapor:melt ratio was large – i.e., crystallization was nearly complete. Upon reaching and reequilibrating with the melt-rich horizon, the vapor became enriched in carbon. With cooling graphite precipitated, and the residual vapor was again driven to more H_2O-rich compositions (Mathez et al. 1989).

Hydration and remelting of the protoreef. Hydration of intercumulus melt in the protoreef must have been accompanied by melting of the crystalline assemblage. How this happened can be established only generally from available experimental data. The addition of water to mafic melt has three major effects: (1) olivine is stabilized at the expense of pyroxene (e.g., Kushiro et al. 1968); (2) plagioclase stability is depressed relative to the mafic silicate minerals (e.g., Holloway and Burnham 1972; Helz 1976; Rutherford et al. 1985); and (3) spinel stability is enhanced relative to the silicate phases (Ford et al. 1972).

The experiments most directly applicable to the present case are those of Ford et al. (1972), who investigated the melting behavior of Apollo 14 high-alumina basalt 14310. The phase relations are illustrated in Fig. 10a. It can be seen that the combined effects of increased water content and pressure are to change the paragenetic sequence from plagioclase – Cr-spinel – olivine – pyroxene at 1 atm to Cr-spinel – plagioclase – olivine – pyroxene at 2 kbar to Cr-spinel – olivine – plagioclase – pyroxene at 5 kbar. The pseudoternary projection of Fig. 10b further illustrates that the reaction points migrate away from both the olivine apex *and* the plagioclase-olivine join, displacing the cotectics upward and enlarging the stability field of spinel.

Sample 14310 contains ≈48% SiO_2, 20% Al_2O_3, 8% MgO and 12% CaO and is thus unlike any conceivable Bushveld intercumulus melt, which coexisted with orthopyroxene and plagioclase and thus must have been more siliceous and magnesian and less calcic. In addition, the

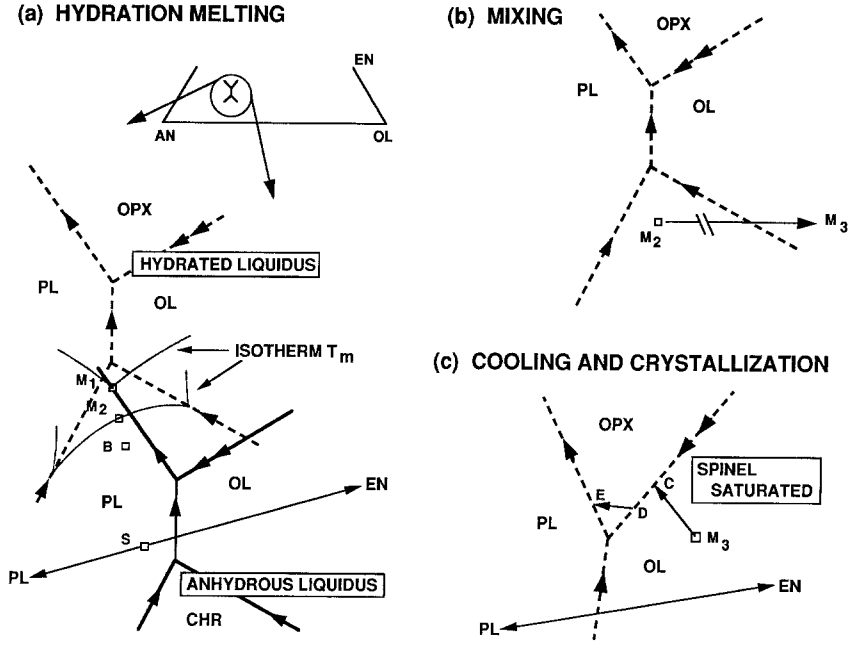

Fig. 11a–c. An interpretation for the Merensky reef by hydration melting: **a** Schematic liquidus relationships projected as in Fig. 10b. M_1 is the composition of the initially anhydrous intercumulus melt in the norite at temperature T_m; M_2, the hydrated, chromite-saturated melt at the same temperature; B, the bulk composition of the norite protolith; S, the bulk composition of the protolith crystalline assemblage. The isotherm T_m is traced on the anhydrous (*solid*) and hydrous (*dashed*) liquidi. The observed sequence norite – anorthosite – chromitite – pegmatoid records the position of the melting/hydration front. **b** Melt M_2 mixes with that produced by melting of the hanging wall. The mixture, M_3, is off the plane of the cotectics and in the olivine+spinel field of stability. **c** With cooling, M_3 crystallizes along the path M_3-C-D-E. It remains spinel-saturated during crystallization of the silicates

composition of the intercumulus melt must have been at or near the orthopyroxene – chromite boundary curve (see below), which is not present in the compositional space represented by high-alumina basalt. It is emphasized that the effect of water on the crystallization behavior of Bushveld magma is not well-constrained by the Ford et al. or any other experimental studies, and therefore it is possible only to rationalize the observations of the rocks with knowledge from experiments.

One interpretation for the formation of the lithologic sequence through the Merensky Reef permitted by the experiments and consistent with the observations is presented in Fig. 11. Consider the isothermal hydration of intercumulus melt at temperature T_m (Fig. 11a). The composition of the initial melt (M_1) in norite is constrained to lie on the anhydrous plagioclase – orthopyroxene cotectic (heavy solid lines), and the bulk composition (B) of the partially molten norite is somewhere between M_1 and the bulk solid composition (S). Assume that with hydration the cotectics (dashed for the hydrated system) are shifted in the manner shown. As hydration progresses, first orthopyroxene dissolves, leaving the system saturated only in plagioclase. With continued hydration the proportion of melt increases as plagioclase dissolves and eventually the melt becomes chromite-saturated (M_2). Note that M_2 remains on isotherm T_m.

Thus the observed reef footwall sequence of norite – anorthosite – chromitite – pegmatoid (i.e., hydrated melt) records the sequence of mineral stabilities present during isothermal hydration across the hydration front. The front must have been accompanied by concentration gradients in other melt components generated in response to selective mineral dissolution or crystallization, as discussed further below, and thus the sequence formed in a manner analogous to the formation of metamorphic blackwalls around ultramafic bodies (e.g., Sanford 1982). The hydration front and sequence of mineral stabilities progressed down into the footwall as water was added to the melt-rich protoreef, but eventually this process ceased as water and thus the heat required for fusion was exhausted.

The hydration/melting front also migrated upward into the pyroxenite hanging wall. The pyroxenite contains minor chromite, constraining the composition of intercumulus melt to the orthopyroxene – spinel boundary. The nature of this boundary and the behavior of compositions close to it are not well established. However, there are natural melts in which spinel and pyroxene coexist. For example, Stolper (1977) showed that liquidi of natural eucritic meteorites are multiply saturated in olivine, pigeonite, plagioclase and spinel – i.e., the two reaction points shown on Fig. 11a merge. Eucrites contain as major phases low-Ca pyroxene and calcic plagioclase, with Cr-spinel being a "minor but ubiquitous phase", so they are a good analogue for the Merensky pegmatoid.

Based on the melting behavior of 14310 it is speculated that hydration displaced the orthopyroxene – spinel boundary such that the intercumulus melt in the pyroxenite became saturated only in spinel, resulting in the melting of orthopyroxene, upward migration of the melting/hydration front and the formation of the upper chromitite in a manner analogous to the lower one. An important consequence of melting of both hanging wall and footwall was that the composition of the intervening hydrated melt was shifted to an intermediate composition. This is illustrated in Fig. 11b. Here melt M_2 produced by melting the footwall mixes with enstatite-rich melt from the hanging wall to produce mixture M_3, which is shifted to the field of olivine+spinel stability. M_3 represents the bulk composition of the model Merensky pergmatoid. *It is not on the same composition plane as the phase boundaries* of Fig. 11a, b because upon cooling the melt remains saturated in spinel as other phases crystallize. The relevant phase relations for M_3 are schematically portrayed in Fig. 11c, which also illustrates

how the Merensky pegmatoid crystallized. The spinel-saturated melt evolved along the path M_3-C-D-E, yielding rocks in which olivine is partially to completely resorbed and which exhibit the paragenetic sequence chromite + olivine – orthopyroxene – plagioclase.

Discussion

Chromite compositional gradients. The compositional gradient in the melt across the hydration front is now preserved as the systematic variation of chromite composition. Thus, the higher Al/R3 of chromite in seams adjacent to norite or anorthosite compared to that of chromite in the pegmatoid or in seams adjacent to pyroxenite is interpreted to be due to plagioclase melting, which supplied Al to chromite. The trends of increasing Al/R3 across chromitite seams toward adjacent norite and anorthosite also reflect gradients in melt Al contents.

Variations in reef lithology. The different reef facies can be placed in an evolutionary scheme determined by the degree to which the melt – crystal reactions occurred, which in turn depended on the amount of water added and the degree to which the generated melt was lost.

The fine-grained pyroxenite of section TP represents the original cumulus hanging wall to which insufficient water was added to cause significant melting, and thus the chromitite and anorthosite layers are missing. In section BP1A, the rare pegmatoidal orthopyroxene in the otherwise fine-grained pyroxenite indicates that remelting was halted at its inception, perhaps because little water reached this part of the reef. Thus, the bottom chromitite seam is barely developed and lacks an accompanying anorthosite layer. In sections BN and BP1B the pegmatoidal pyroxenite is well developed but inclusions of fine-grained pyroxenite are present because remelting was incomplete. Only thin anorthosite and chromitite seams are present at the bottom contact and a discontinuous chromitite seam is present at the top contact. In the TN section the process proceeded further, resulting in the full development of pegmatoid bounded on both sides by well-developed chromitites and a lower anorthosite layer.

It is hypothesized that the different bulk compositions, represented by the range of olivine-free to olivine-rich lithologies, originated from the same initial protolith and that the proportion of olivine preserved in the reef was determined by the extent to which the melt generated by hydration was subsequently lost. The pegmatoidal feldspathic pyroxenite reef facies represents the bulk composition M_3 (Fig. 11c), the olivine having reacted peritectically back to orthopyroxene. The pegmatoidal harzburgite to dunite facies developed in areas where variable proportions of fractionated melt were lost during crystallization.

Mass balance considerations. The relative amounts of hanging wall and footwall which melted to produce the reef can be calculated from modal data. A mixture of 76% hanging wall (80% pyroxene + 17% plagioclase) and 24% footwall (19% pyroxene + 76% plagioclase) gives a rock of 65% pyroxene and 31% plagioclase, which approximates the reef pegmatoid.

One problem is to account for the Cr now held in the Merensky Reef as chromite. Reef and hanging-wall orthopyroxene contains $\approx 0.45\%$ Cr_2O_3 and footwall orthopyroxene $\approx 0.30\%$ Cr_2O_3. Assuming that the pyroxenite protolith initially contained 2% chromite and that three times as much hanging wall as footwall melted, then 49 cm of the hanging wall and 16 cm of the footwall are required to account for 20 cm of pegmatoid with 3.6% disseminated chromite and two 0.5 cm-thick chromitite seams. Although these estimates are obviously sensitive to input parameters, changing them has little effect on the conclusion that to account for reef chromite requires hydration melting of a larger mass of rock than represented by the pegmatoid. It would appear that either a significant amount of melt was lost from the horizon of hydration melting or that the protolith contained much more than 2% chromite.

Formation of potholes. If fluid was introduced through fractures in the underlying rocks, then the protoreef in regions where there were relatively numerous fractures would have been supplied with more fluid than elsewhere. Here the hydration and accompaning reaction front moved further downward into the footwall, forming the potholes. Thus, potholes are envisioned as products of chemical erosion. They are post-cumulus features that formed by the same mechanism as the rest of the reef except that the overlying rocks sagged into and displaced some of the hydrated melt in the pothole depressions. The idea that potholes mark the injection of fluid has also been suggested by Kinloch (1982), Elliot et al. (1982) and Kinloch and Peyerl (1990). Other models for their formation have invoked mechanical or thermal erosion (Irvine et al. 1983; Buntin et al. 1985; Campbell 1986) or non-deposition during crystallization of foot wall units (Ballhaus 1988). Whether or not chemical erosion can better account for characteristics of potholes must await further study.

Comparison with the Stillwater Howland Reef. This model for the Merensky Reef is analogous to one developed by Boudreau (1988) for the Howland Reef of the Stillwater Complex. Boudreau reported anorthosite layers and chromite-bearing rocks surrounding olivine pegmatoids. He proposed that the mafic components from the adjacent cumulates were leached and migrated into water-rich pockets and that plagioclase in the reaction zone dissolved incongruently and was reprecipitated, thereby forming the pegmatoids and anorthosites. Mafic/felsic segregation in the Merensky Reef is, in effect, represented by the anorthosite layer at the reef – norite interface. Here the segregation process was less extreme than in the Howland Reef, as indicated by the fact that the Merensky pegmatoid itself is relatively feldspathic ($\approx 30\%$ plagioclase).

Boudreau proposed that Cr released from orthopyroxene melting caused precipitation of chromite, which

was preferentially concentrated at the margins of the fluid-rich zone. He argued that chromite is relatively unstable at high H_2O fugacity based on the observation that modal chromite is inversely correlated with modal phlogopite. However, in the Merensky rocks chromite is most abundant in samples containing high modal proportions of phlogopite, and the experimental data (Fig. 10) clearly indicate that chromite is relatively more stable than mafic silicates with increasing P_{H_2O}. Given that chromite stability is particularly sensitive to melt Al contents, the seemingly inconsistent behavior of chromite in the Stillwater and Bushveld rocks could be due to slight differences in compositions of the intercumulus melts and the specific reactions they underwent with the crystalline assemblage. Thus melts in the two intrusions would have followed somewhat different paths through Fig. 11.

Conclusion

The Merensky Reef is magmatic but not cumulate. It formed in a partially molten cumulate pile by hydration and consequent isothermal melting of an initially melt-rich horizon. Hydration occurred by introduction of vapor through fractures in the footwall. The fractures were unable to propagate through the melt-rich protoreef, and H_2O from the vapor was absorbed by the H_2O-undersaturated melt, leaving a residual vapor enriched in carbon species. The composition of the melt was initially confined to the orthopyroxene – plagioclase cotectic by the crystalline assemblage. Melting due to hydration occurred first by resorption of orthopyroxene. With continued hydration and the disappearance of orthopyroxene, plagioclase began to melt. Eventually, the melt migrated to the stability field of chromite, the stabilization of which was a result of the increase in melt alumina due to plagioclase resorption. The stratigraphic sequence downward through the base of the reef of pegmatoidal feldspathic pyroxenite (hydrated melt) – chromitite – anorthosite – norite thus represents the sequence of stable mineral assemblages from high- to low-H_2O contents through the hydration/melting front. The gradient in H_2O content thus also was accompanied by gradients in other melt components, such as alumina, which now are reflected in well-defined variations in chromite compositions. This sequence of mineral stabilities through the hydration front is consistent with knowledge of melting behavior derived from experimental investigations. Hydration melting of the norite footwall and pyroxenite hanging wall produced a mixed melt that upon cooling remained spinel-saturated as it crystallized in the order olivine – orthopyroxene – plagioclase and is now represented by the Merensky pegmatoid. Mass balance considerations require that a significant proportion of the hydrated intercumulus melt was lost.

In addition to accounting for the typical lithologic sequence of the Rustenburg section of the Merensky Reef and for the regular variations in chromite compositions, the model also accounts for the variations in reef lithology along strike. Thus, well-developed pegmatoid is accompanied by well-developed chromitite seams and a basal anorthosite layer. Inclusions of rock identical to the hanging-wall pyroxenite and footwall norite are present in the pegmatoid and represent remnants of its prōtolith that survived hydration melting. Where the pegmatoid is less well-developed, so too are the bounding chromitite seams, and the thickness of the basal chromitite and underlying anorthosite layers are related in a positive manner. Lithologies ranging from feldspathic pyroxenite to dunite originated from the same protolith. The proportion of olivine preserved was determined by the extent to which the melt generated by hydration was lost. Potholes formed where the melting process penetrated relatively deep into the footwall stratigraphy.

The concentration of PGEs in the Merensky Reef can be rationalized by either accumulation of magmatic sulfides from overlying magma in the protoreef or by transport of PGEs in, and subsequent deposition from, the vapor that initiated hydration and melting.

Acknowledgements. This work was made possible by the access to the mines provided by Johannesburg Consolidated Investment Company Ltd., by the guidance of C.A. Lee, by the thoughtful reviews of the manuscript by R.G. Cawthorn, A.E. Boudreau, J. Longhi, D. Walker, R. Hutchinson, C.A. Lee and R.T. Brown, by the logistical support and hospitality of T.G. Molyneux and G. Chunnet and by the financial support provided by NSF grants EAR8409834 and EAR8720982 and The University of Washington Graduate School Research Fund. We thank these individuals and institutions for their help.

References

Allan JF, Sack RO, Batiza R (1988) Cr-rich spinels as petrogenetic indicators: MORB-type lavas from the Lamont seamount chain, eastern Pacific. Am Mineral 73:741–753

Ballhaus CG (1988) Potholes of the Merensky Reef at Brakspruit Shaft, Rustenburg Platinum Mines; primary disturbance in the magmatic stratigraphy. Econ Geol 83:1140–1158

Ballhaus CG, Stumpfl EF (1985) Occurrence and petrologic significance of graphite in the Upper Critical Zone, western Bushveld Complex, South Africa. Earth Planet Sci Lett 74:58–68

Ballhaus CG, Stumpfl EF (1986) Sulfide and platinum mineralization in the Merensky Reef: evidence from hydrous silicates and fluid inclusions. Contrib Mineral Petrol 94:193–204

Barnes SJ (1986) The effect of trapped liquid crystallization on cumulus mineral compositions in layered intrusions. Contrib Mineral Petrol 93:524–531

Barnes SJ, Campbell IH (1988) Role of late magmatic fluids in Merensky-type platinum deposits: a discussion. Geology 16:488–491

Barnes SJ, Naldrett AJ (1985) Geochemistry of the J-M (Howland) Reef of the Stillwater Complex, Minneapolis adit area. I. Sulfide chemistry and sulfide-olivine equilibrium. Econ Geol 80:627–645

Boudreau AE (1986) The role of fluids in the petrogenesis of platinum-group element deposits in the Stillwater Complex, Montana. Unpubl PhD Dissertation, University of Washington

Boudreau AE (1988) Investigations of the Stillwater Complex. IV. The role of volatiles in the petrogenesis of the J-M reef, Minneapolis adit section. Can Mineral 26:193–208

Boudreau AE, Mathez EA, McCallum IS (1986) Halogen geochemistry of the Stillwater and Bushveld Complexes: evidence for transport of the platinum-group elements by Cl-rich fluids. J Petrol 27:967–986

Brynard HJ, De Villiers JPR, Viljoen EA (1976) A mineralogical

investigation of the Merensky Reef at the Western Platinum Mine, near Marikana, South Africa. Econ Geol 71:1299–1307

Buntin TJ, Grandstaff DE, Ulmer GC, Gold DP (1985) A pilot study of geochemical and redox relationships between potholes and adjacent normal Merensky Reef of the Bushveld Complex. Econ Geol 80:975–987

Cameron EN, Desborough GA (1969) Occurrence and characteristics of chromite deposits – eastern Bushveld Complex. Econ Geol Monogr 4:23–40

Campbell IH (1986) A fluid dynamic model for the potholes of the Merensky Reef. Econ Geol 81:1118–1125

Campbell IH, Naldrett AJ, Barnes SJ (1983) A model for the origin of the platinum-rich sulfide deposits in the Bushveld and Stillwater Complexes. J Petrol 24:133–165

Cousins CA (1964) The platinum deposits of the Merensky Reef. In: Haughton SH (ed) The geology of some ore deposits of southern Africa. (Vol II) Geol Soc S Afr, Johannesburg, pp 225–237

Cousins CA (1969) The Merensky Reef of the Bushveld Igneous Complex. Econ Geol Monogr 4:239–251

Eales HV (1987) Upper Critical Zone chromitite layers at R.P.M. Union section mine, western Bushveld complex. In: Stowe CW (ed) Evolution of chromium ore fields. Van Nostrand Reinhold Co, New York, pp 144–168

Eales HV, Reynolds IM (1986) Cryptic variations within chromitites of the upper Critical Zone, northwest Bushveld Complex. Econ Geol 81:1056–1066

Elliott WC, Grandstaff DE, Ulmer GC, Buntin T, Gold DP (1982) An intrinsic oxygen fugacity study of platinum-carbon associations in layered intrusions. Econ Geol 77:1493–1510

Farquhar J (1986) The Western Platinum Mine. In: Anhaeusser CR, Maske S (eds) Mineal deposits of South Africa. Geol Soc S Afr, Johannesburg, pp 1135–1142

Fleet ME, MacRae ND (1988) Partition of Ni between olivine and sulfide: equilibria with sulfide-oxide liquids. Contrib Mineral Petrol 100:462–469

Fisk MR, Bence AE (1980) Experimental crystallization of chrome spinel in FAMOUS basalt 527-1-1. Earth Planet Sci Lett 48:111–123

Ford CE, Biggar GM, Humphries DJ, Wilson G, Dixon D, O'Hara MJ (1972) Role of water in the evolution of the lunar crust; an experimental study of sample 14310; an indication of lunar calc-alkaline volcanism. Proc Lunar Sci Conf 3rd:207–229

Hamlyn PR, Keays RR (1979) Origin of chromite compositional variation in the Panton Sill, Western Australia. Contrib Mineral Petrol 69:75–82

Hatton CJ, von Gruenewaldt G (1985) Chromite from the Zwartkop Chrome Mine – an estimate of the effects of subsolidus reequilibration. Econ Geol 80:911–924

Helz RT (1976) Phase relations of basalts in their melting ranges at $P_{H_2O}=5$ kbar, part II. melt compositions. J Petrol 17:139–193

Henderson P (1975) Reaction trends shown by chrome-spinels of the Rhum layered intrusion. Geochim Cosmochim Acta 39:1035–1044

Henderson P, Suddaby P (1971) The nature and origin of the chrome-spinel of the Rhum layered intrusion. Contrib Mineral Petrol 33:21–31

Hill RL, Sack RO (1987) Thermodynamic properties of Fe-Mg titanomagnetite spinels. Can Mineral 25:443–464

Holloway JR, Burnham CW (1972) Melting relations of basalt with equilibrium water pressure less than total pressure. J Petrol 13:1–29

Irvine TN (1967) Chromian spinel as a petrogenetic indicator, part 2. petrologic applications. Can J Earth Sci 4:71–103

Irvine TN, Keith DW, Todd G (1983) The J-M platinum-palladium reef of the Stillwater Complex, Montana: II. origin by double-diffusive convective magma mixing and implications for the Bushveld Complex. Econ Geol 78:1287–1334

Jackson ED (1969) Chemical variation in coexisting chromite and olivine in chromitite zones of the Stillwater Complex. Econ Geol Monogr 4:41–75

Kinloch ED (1982) Regional trends in the platinum-group mineralogy of the Critical Zone of the Bushveld Complex, South Africa. Ecol Geol 77:1328–1347

Kinloch ED, Peyerl W (1990) Platinum-group minerals in various types of Merensky Reef: genetic implications. Econ Geol 85:537–555

Kruger FJ, Marsh JS (1982) Significance of $^{87}Sr/^{86}Sr$ ratios in the Merensky cyclic unit of the Bushveld Complex. Nature 298:53–55

Kruger FJ, Marsh JS (1985) The mineralogy, petrology, and origin of the Merensky cyclic unit in the western Bushveld Complex. Econ Geol 80:958–974

Kushiro I, Yoder HS Jr, Nishikawa M (1968) Effect of water on the melting of enstatite. Geol Soc Am Bull 79:1685–1692

Lauder WR (1970) Origin of the Merensky Reef. Nature 227:365–366

Leeb-du Troit A (1986) The Impala Platinum Mines. In: Anhaeusser CR, Maske S (eds) Mineral deposits of South Africa. Geol Soc S Afr, Johannesburg, pp 1091–1106

Mathez EA (1989) The nature of vapor associated with mafic magma and controls on its composition. In: Whitney JA, Naldrett AJ (eds) Ore deposition associated with magmas. Rev Econ Geol 4:21–31

Mathez EA, Dietrich VJ, Holloway JR, Boudreau AE (1989) Carbon distribution in the Stillwater Complex and evolution of vapor during crystallization of Stillwater and Bushveld magmas. J Petrol 30:153–173

McCallum IS (1968) Equilibrium relationships between the coexisting minerals in the Stillwater Complex, Montana. Unpubl PhD Dissertation, University of Chicago

McCallum IS, Raedeke LD, Mathez EA (1977) Stratigraphy and petrology of the Banded Zone of the Stillwater Complex, Montana (abstract). EOS 58:1245

Mostert AB, Hofmeyr PK, Potgieter GA (1982) The platinum-group mineralogy of the Merensky Reef at the Impala Platinum mines, Bophuthatswana. Econ Geol 77:1385–1394

Naldrett AJ, Gasparini EC, Barnes SJ, von Gruenewaldt G, Sharpe MR (1986) The Upper Critical Zone of the Bushveld Complex and the origin of Merensky-type ores. Econ Geol 81:1105–1117

Nicholson DM (1989) The petrogenesis of the Merensky Reef, Bushveld Complex. Unpubl MS Thesis, University of Washington

O'Hara MJ (1968) The bearing of phase equilibria studies in synthetic and natural systems on the origin and evolution of basic and ultrabasic rocks. Earth-Sci Rev 4:69–133

Rutherford MJ, Sigurdsson H, Carey S, Davis A (1985) The May 18, 1980, eruption of Mount St. Helens, 1, melt composition and experimental phase equilibria. J Geophys Res 90:2929–2947

Sack RO (1982) Spinels as petrogenetic indicators: activity – composition relations at low pressures. Contrib Mineral Petrol 79:169–182

Sanford RF (1982) Growth of ultramafic reaction zones in greenschist to amphibolite facies metamorphism. Am J Sci 282:543–616

Schmidt ER (1952) The structure and composition of the Merensky Reef and associated rocks in the Rustenburg Platinum Mine. Trans Geol Soc S Afr 55:233–279

Sharpe MR (1985) Strontium isotope evidence for preserved density stratification in the main zone of the Bushveld Complex, South Africa. Nature 316:119–126

Stolper E (1977) Experimental petrology of eucritic meteorites. Geochim Cosmochim Acta 41:587–611

Vermaak CF (1976) The nickel pipes of Vlakfontein and vicinity, western Transvaal. Econ Geol 71:261–286

Viljoen MJ, Hieber R (1986) The Rustenburg Section of Rustenburg Platinum Mines Limited, with reference to the Merensky

Reef. In: Anhaeusser CR, Maske S (eds) Mineral deposits of South Africa. Geol Soc S Afr, Johannesburg, pp 1107–1134
Viljoen MJ, De Klerk WJ, Coetzer PM, Nash NP, Kinloch E, Peyerl W (1986a) The Union Section of Rustenburg Platinum Mines Limited, with reference to the Merensky Reef; In: Anhaeusser CR, Maske S (eds) Mineral deposits of South Africa. Geol Soc S Afr, Johannesburg, pp 1061–1090
Viljoen MJ, Theron J, Underwood B, Walters BM, Weaver J, Peyerl W (1986b) The Amandelbult Section of Rustenburg Platinum Mines Limited, with reference to the Merensky Reef. In: Anhaeusser CR, Maske S (eds) Mineral deposits of South Africa. Geol Soc S Afr, Johannesburg, pp 1041–1060
Volfinger M, Robert J-L, Vielzeuf D, Neiva AMR (1985) Structural control of the chlorine content of OH-bearing silicates (micas and amphiboles). Geochim Cosmochim Acta 49:37–48
Walker D, Jurewicz S, Watson EB (1988) Adcumulus dunite growth in a small thermal gradient. Contrib Mineral Petrol 99:306–319

Editorial resposibility: I.S.E. Carmichael